2012-04-05

Magnetic structure variation in manganese-oxide clusters

Hooper, Joseph P.

American Institute of Physics

K. S. Williams, J. P. Hooper, J. M. Horn, J. M. Lightstone, H. Wang, Y. J. Ko, and K. H. Bowen. "Magnetic structure variation in manganese-oxide clusters." J. Chem. Phys. 136, 134315 (2012)
http://hdl.handle.net/10945/48675

Magnetic structure variation in manganese-oxide clusters

Kristen S. Williams,[1,2] Joseph P. Hooper,[3,a)] Jillian M. Horn,[2] James M. Lightstone,[2] Haopeng Wang,[4] Yeon Jae Ko,[4] and Kit H. Bowen[4]
[1]*Materials Science and Engineering Program, Texas A&M University, College Station, Texas 77843, USA*
[2]*Research Department, Naval Surface Warfare Center, Indian Head, Maryland 20640, USA*
[3]*Department of Physics, Naval Postgraduate School, Monterey, California 93943, USA*
[4]*Departments of Chemistry and Materials Science, Johns Hopkins University, Baltimore, Maryland 21218, USA*

(Received 12 February 2012; accepted 12 March 2012; published online 5 April 2012)

Negative-ion photoelectron spectroscopy and *ab initio* simulations are used to study the variation in magnetic structure in Mn_xO_y ($x = 3, 4$; $y = 1, 2$) clusters. The ferrimagnetic and antiferromagnetic ground-state structures of Mn_xO_y are 0.16–1.20 eV lower in energy than their ferromagnetic isomers. The presence of oxygen thus stabilizes low-spin isomers relative to the preferred high-spin ordering of bare Mn_3 and Mn_4. Each cluster has a preferred overall magnetic moment, and no evidence is seen of competing states with different spin multiplicities. However, non-degenerate isomags, which possess the same spin multiplicity but different arrangements of local moments, do contribute additional features and peak broadening in the photoelectron spectra. Proper accounting for all possible isomags is shown to be critical for accurate computational prediction of the spectra.
 [http://dx.doi.org/10.1063/1.3698279]

INTRODUCTION

Magnetic clusters exist on a scale where impurities result in significant changes in bonding, overall moments, and spin orientation. Manganese, with an electronic configuration of $3d^5 4s^2$, has a half-filled d shell which gives rise to a magnetic moment of 5 μ_B per atom. The coupling between Mn atoms is relatively weak, allowing for a wide variation in magnetic properties and significant sensitivity to impurities at the molecular scale. Numerous theoretical and experimental studies have examined the magnetic structure in pure manganese clusters.[1–8] The magnetic ordering of the Mn_2 dimer is very sensitive to interatomic separation,[1–3] while clusters containing 3–5 Mn atoms are all predicted to have ferromagnetic ground states with magnetic moments of ∼5 μ_B/atom.[2,4,5] Mn_6 and Mn_7 are ferrimagnetic,[5,9] and there is a distinct transition from high- to low-spin configurations in Mn_n clusters with $n \geq 7$.[5] In all anionic clusters, Mn_n^- ($n = 2$–8), the preferred ordering is ferromagnetic.[7]

The addition of a single oxygen into certain bare Mn clusters has also been considered.[3,10–13] Previous work on Mn_2O (Ref. 10) employed experimental negative-ion photoelectron spectroscopy (PES) and *ab initio* calculations to study the effect of oxygen on the magnetic properties of the Mn_2 dimer. It was found that the presence of one additional O atom both strengthens cluster binding energy and alters the Mn-Mn magnetic coupling. In bare Mn_2 with a manganese spacing larger than 3.06 Å, the high-spin state with a moment of 10 μ_B is preferred,[1,2] and the low-spin state with $S = 0$ is ∼5 eV higher in energy.[3] The addition of oxygen reduces this gap, leading to nearly degenerate ferromagnetic and antiferromagnetic states in the Mn_2O anion.[10] Both isomers of Mn_2O^- contribute to peak broadening in the experimental PES and must be included in calculations to accurately reproduce the spectral peak positions and shapes.

Mn_5O and Mn_6O were studied by Jones *et al.* using a combination of negative-ion PES and quantum calculations.[11] They found that the ferromagnetic states of Mn_5 and Mn_6 are destabilized by the addition of oxygen, and the overall magnetic moment is reduced compared to pure Mn_n clusters. Another conclusion of this work was the identification of several nearly degenerate "isomags." Akin to structural isomers, isomags are magnetic isomers with comparable binding energies and identical spins but different distributions of local moments. Because of weak magnetic exchange interactions between Mn moments, there is a small barrier to spin reorientation which is strongly affected by changes in Mn-Mn interatomic separation and atomic composition.[1,3,14] As a result, Mn_5O^- and Mn_6O^- display a number of magnetic isomers, each with a subset of possible isomags.[11] The authors further conclude that the presence of multiple peaks in the PES spectra can only be accounted for by including contributions from all isomers and their corresponding isomags. Reasonable agreement between theory and the experimental vertical detachment energies in the PES spectra were observed, though for Mn_5O^- and Mn_6O^- a constant energy shift was required to accurately reproduce the experimental peaks.

In this work, we present a combined experimental and theoretical study that explores the effects of oxygen content on the magnetic properties of Mn_3 and Mn_4 clusters. Small Mn_xO_y ($x = 3, 4$; $y = 1, 2$) clusters are characterized via negative-ion photoelectron spectroscopy and analyzed with *ab initio* calculations of the structure, magnetic order, and vertical detachment energies (VDEs).

The experimentally measured VDEs correspond to the energy difference between the anion and the neutral cluster

a)Electronic mail: jphooper@nps.edu.

with the latter fixed at the anion geometry. The anion's electron is ejected via photoionization and the electronic structure rapidly relaxes to a new state. The kinetic energy of the ejected electron (EKE) is measured experimentally via PES, and the electron binding energy (EBE) is derived from knowledge of the incident photon energy via the conservation equation

$$\mathrm{EBE} = h\nu - \mathrm{EKE}, \tag{1}$$

where ν is the laser frequency. The resulting binding energies are compared with atomic-level simulations, offering a direct comparison to theoretical calculations of small atomic clusters. This combined experimental-theoretical approach has been shown to successfully identify the ground state of gas-phase clusters with nearly degenerate magnetic states.[15]

Ground-state geometries and magnetic structures for all clusters were calculated and validated experimentally by comparison with the experimental spectra. Good agreement was observed between the ground-state VDEs of the lowest energy cluster geometries and the prominent PES features, with no energy shift required to match the main spectral peaks. The addition of oxygen reduces the net magnetic moment and stabilizes different magnetic ground states compared to Mn_3 and Mn_4. Calculations of transitions from the anion to excited states of the neutral show reasonable agreement with higher order and secondary peaks in the structure. For all systems considered, only a single magnetic isomer appears to be observed in the experimental PES, though transitions to various isomags of this single isomer do appear to contribute significantly.

COMPUTATIONAL METHODOLOGY

All calculations were performed with spin-unrestricted density functional theory (DFT) using the PBE functional for both exchange and correlation. A large aug-cc-pvdz basis set was used, and all simulations were performed using GAUSSIAN 09 (Ref. 16) at the Air Force Research Laboratory (AFRL) supercomputing center. Global energy minima for all clusters were found by considering a large number of possible configurations and oxygen locations; only the lowest energy structures (those with contributions to the experimental spectra) are presented. This methodology was validated by successfully reproducing previous structures and VDEs for Mn_2O^- [Ref. 10].

One critical aspect of calculations on these clusters is a careful description of the magnetic ordering. We consider all possible spin isomers for each cluster, identifying them by the following naming convention. Ferromagnetic (FM) indicates that all Mn magnetic moments are parallel (i.e., a high-spin cluster). Antiferromagnetic (AFM) indicates that equal numbers of Mn moments are aligned in the opposite direction, and the net cluster moment is zero. Finally, fM indicates ferrimagnetic ordering where more moments are aligned parallel than anti-parallel; the result is a reduced, but non-zero spin moment. Only clusters with AFM or fM ordering can have multiple non-degenerate isomags. These are treated with a multistep approach, in which spin orientation (but not magnitude) is fixed and the wavefunction is checked for magnetic instabilities during the course of the geometry optimization.

Once the lowest energy isomags are identified for the anionic clusters, the vertical detachment energies are calculated; these correspond to transitions to the neutral cluster with a multiplicity of $M \pm 1$. The VDEs are defined as the differences in the single point energies of the anions and neutral clusters, with the latter fixed at the optimized anion geometry. Higher order peaks in the PES are compared to excited states of the neutral cluster, but with the geometry and spin configuration still held fixed at the ground-state orientation. The excited-state energies are calculated using time-dependent density functional theory (TD-DFT), again with the aug-cc-pvdz basis set. Finally, an adiabatic electron affinity (AEA) for each cluster is estimated by calculating the energy difference between the optimized, lowest energy isomags of both the anion and neutral. This differs from the VDE calculations in that both the structural parameters and magnetic structure of the neutral cluster are allowed to relax. This allows for the possibility of transitions to additional structural isomers with potentially different multiplicities. This characteristic is unique to clusters with multiple spin moments, and the effect is discussed further in Experimental Method and Results and Discussion sections.

EXPERIMENTAL METHOD

Negative-ion photoelectron spectroscopy is conducted by crossing a mass-selected beam of negative ions with a photon beam of known frequency. In the experimental apparatus, mass-selection of the desired clusters is achieved by time-of-flight mass spectrometry. The photon beam is derived from the third harmonic of a Nd:YAG laser, giving the incident photons an energy of 3.49 eV. Beams of Mn_xO_y ($x = 2$–8; $y = 1, 2$) are generated by laser ablating and/or spark eroding a rotating, translating manganese rod while pulsing from above with oxygen-doped helium gas. The energy of the photodetached electrons is measured by a magnetic bottle analyzer, and the final kinetic energies are converted to binding energies for each cluster. The spectral resolution is $\sim$50 meV at EKE = 1 eV. Experimental data are plotted as intensity (or counts) versus binding energy. All experiments were performed at Johns Hopkins University, and the apparatus is described in detail elsewhere.[17,18]

RESULTS AND DISCUSSION

The ground state for each manganese oxide cluster is found by calculating cluster energy as a function of spin multiplicity. We calculate all allowed multiplicities for different starting geometries of each cluster to determine the overall lowest energy configuration. Figures for the corresponding ground states appear in the following subsections; bond lengths are given in Å, while magnetic moments on the Mn atoms (shown in italics) have units of μ_B. The magnetic moments of O atoms are small relative to those of the manganese, generally of the order of 0.1 μ_B. These contribute little to the net cluster moment and thus are not shown in the figures. As discussed below, the presence of the O atoms slightly alters

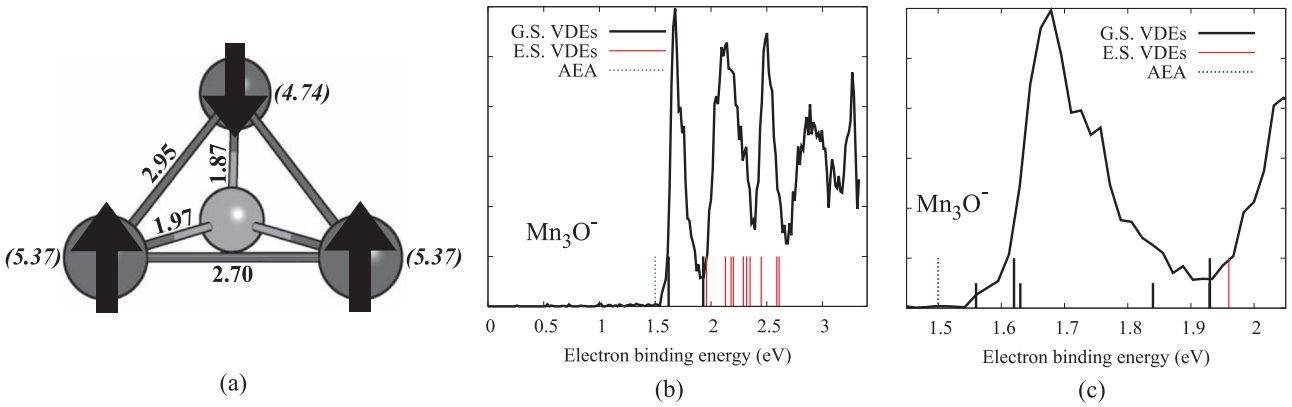

FIG. 1. (a) Ground-state structure of Mn_3O^-. (b) Experimental and theoretical PES for Mn_3O^- (solid line). VDEs for transitions from the ground-state anion to the fixed-geometry, ground-state neutral are shown as black lines, while transitions to the excited states of the fixed-geometry neutral are red. The blue line is the AEA from Table II. (c) Zoomed version of (b) which includes additional VDEs for three higher energy isomags of the neutral cluster (shown as short lines).

the spin moment on adjacent Mn atoms. The more prominent effect from adding oxygen is a change in the orientation of individual spins.

Mn_3O^-

Mn_3O^- possesses several structural isomers, each with two distinct energy minima corresponding to high- and low-spin multiplicities (denoted FM and fM, respectively). A tetrahedral structure with $M = 7$ is the global minimum. This corresponds to ferrimagnetic ordering in which one Mn atom is aligned anti-parallel to the other two. There is an additional local minimum at $M = 17$ corresponding to ferromagnetic ordering with all spins fully aligned; it lies 0.16 eV higher in energy, and its calculated VDEs are well below the onset of the experimental PES spectra. This is a general trend seen in all four clusters; namely, alternate structures or spin configurations of the anion that lie approximately 0.15 eV or higher than the ground state are not observed experimentally. The high-spin isomers for Mn_3O^- and other clusters are detailed in the supplementary material.[19]

The ground-state geometry for Mn_3O^- anion with $M = 7$ is shown in Fig. 1(a). The lone oxygen has a small spin magnitude of 0.09 μ_B, while the overall magnetic moment is 6 μ_B. We note that the optimized geometry of Mn_3O^- does not retain perfect T_d symmetry; rather the tetrahedron is compressed and the symmetry is reduced to C_s. This is a result of the shortened Mn-O bond length, 1.91 Å, which is smaller than the average Mn-Mn bond distance and approaches the Mn-O bond length of Mn_2O^- (1.80 Å).

In the bare, planar Mn_3 cluster, the preferred magnetic ordering is FM, and the cluster moment is 15 μ_B.[2,4,5,7,8] The addition of oxygen alters the Mn-Mn coupling and stabilizes a ferrimagnetic ground state with a reduced moment in Mn_3O^-. The average atomic moment, however, is not significantly altered. As shown in Fig. 1(a), the mean spin moment is 5.16 μ_B, close to the free-atom value of 5 μ_B.

The ground state of Mn_3O^- has exactly one isomag, since there is no preference as to which Mn atom in the plane is anti-parallel. Calculation of the corresponding VDEs is straightforward in this case, as only two vertical transitions have to be considered, 7→6 and 7→8, without regard to which Mn moment is anti-aligned. Figure 1(b) shows the calculated VDEs plotted together with the experimental PES for Mn_3O^-. The black lines designate transitions 7→6 and 7→8, where the geometry of the ground state neutral cluster is held fixed at that of the optimized anion. The red lines indicate transitions to the neutral cluster's excited states, and the blue line is the adiabatic electron affinity. The latter is the energy difference between the optimized anion and optimized neutral and serves as a lower bound for the PES data. The VDEs plotted in Fig. 1(b) are also listed in Table I. The Lowest ground state VDE falls very close to the first prominent peak in the experimental spectra; as listed in Table I, our theoretical value differs from experiment by only 0.06 eV. The second ground state VDE falls approximately 0.16 eV lower than experiment. Higher energy spectral features compare reasonably well with excited state transitions, however, detailed peak assignments are likely not warranted as TD-DFT transition energies are only expected to be accurate within 0.2–0.5 eV.

$Mn_3O_2^-$

The $Mn_3O_2^-$ cluster also has multiple structural isomers. The global minimum is a ferrimagnetic ring structure with $M = 5$, shown in Fig. 2(a). As was the case for Mn_3O^-, the $Mn_3O_2^-$ cluster has a higher energy minimum for

TABLE I. Vertical detachment energies for ground-state $M \pm 1$ transitions in $Mn_xO_y^-$ clusters.

Cluster	Transition	VDE (eV)	Expt. (eV)[a]
Mn_3O^-	7→6	1.62	1.68
	7→8	1.93	2.09
$Mn_3O_2^-$	5→4	2.05	2.01
	5→6	1.66	1.65
Mn_4O^-	12→11	1.92	2.05
	12→13	2.48	2.53
$Mn_4O_2^-$	2→1	1.90	1.97
	2→3	2.39	2.29

[a]Experimental values are estimated from the spectral peaks and have an uncertainty of ±0.1 eV.

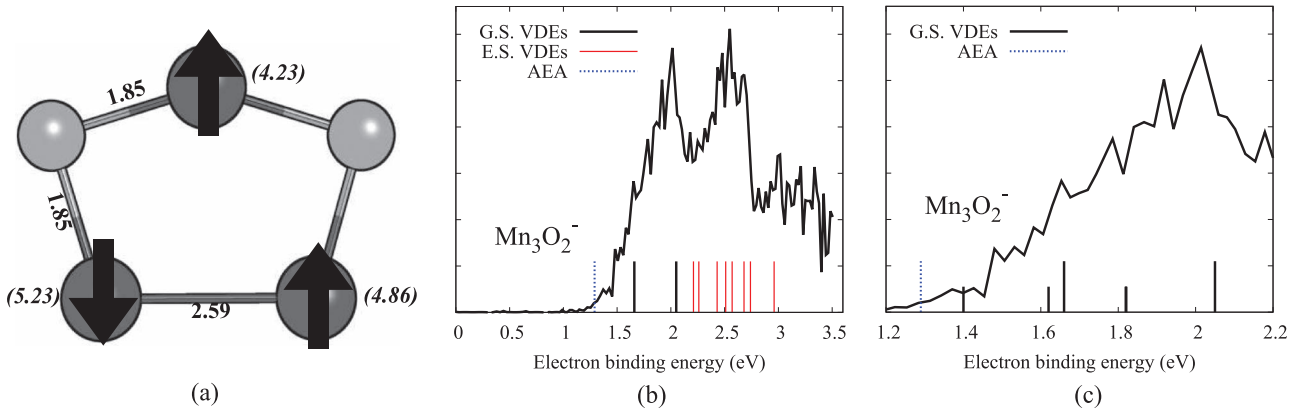

FIG. 2. (a) Ground-state structure and (b) photoelectron spectra of $Mn_3O_2^-$. Notation for the VDEs and the zoomed version (c) is identical to that in Fig. 1.

ferromagnetic ordering at $M = 15$. This structure lies 0.36 eV higher in energy and is shown in the supplementary material.[19] The overall cluster moment of 4 μ_B is reduced compared to that of Mn_3O^- (6 μ_B). The average Mn moment is reduced to 4.77 μ_B, slightly lower than the free-atom value for Mn. Another difference is loss of symmetry and "flattening" of the cluster into a planar C_{2v} configuration.

In the ground state of $Mn_3O_2^-$, one Mn moment is anti-aligned with the other two. The lowest energy isomag corresponds to an anti-parallel moment on a bottom Mn (see Fig. 2(a)). The two isomags with the anti-aligned moment residing on a bottom Mn are equivalent in energy, while the isomag with opposite spin on the top Mn atom is 0.25 eV higher in energy. For calculating VDEs, we must therefore consider $M \pm 1$ transitions (5→4 and 5→6) in which the lowest energy isomag of the anion is used as the starting geometry for the neutral cluster. The experimental PES and calculated VDEs of $Mn_3O_2^-$ are plotted in Fig. 2(b). The first four excited states of the neutral cluster contribute to the higher energy peaks.

Mn_4O^-

The lowest energy cluster of Mn_4O^- is a bipyramid with $M = 12$ and is shown in Fig. 3(a). It has a ferrimagnetic arrangement of spins, and the average Mn moment/atom (from Fig. 3(a)) is 4.97 μ_B. Bare Mn_4 has a tetrahedral structure. Both ferrimagnetic [Ref. 8] and ferromagnetic ground states of Mn_4 have been reported,[2,4,5,7] with the latter having stronger theoretical support. The preferred FM state of Mn_4 is destabilized by the addition of oxygen.

We note that due to the even number of Mn atoms in this cluster, there are two additional local minima which arise from magnetic effects. Namely, there is a minimum for AFM ordering at $M = 2$, in which exactly half of the spins are anti-aligned, and another for FM ordering at $M = 22$, in which all spins are parallel. These alternate spin isomers (given in the supplementary material[19]) are higher in energy than the fM cluster by 0.25 and 0.43 eV, respectively. As in Mn_3O^-, the presence of the shortened Mn-O bond distance compresses the bipyramid, reducing it to C_s symmetry.

For Mn_4O^- in a bipyramid geometry, there are two distinct fM isomags. The ground state configuration with a multiplicity of $M = 12$ corresponds to one of the four Mn moments aligned anti-parallel with the other three. Three of the four isomags contain an anti-aligned Mn moment in the Mn_3 plane. As expected from symmetry, they are equivalent in energy. The fourth isomag has the anti-aligned Mn moment at the apex of the bipyramid. This isomag lies 0.56 eV higher in energy than the in-plane isomags. A separate set of VDEs is calculated for each of the two distinct isomags, and those for the out-of-plane configuration are found to lie below the AEA. Hence, only VDEs for $M \pm 1$ transitions from

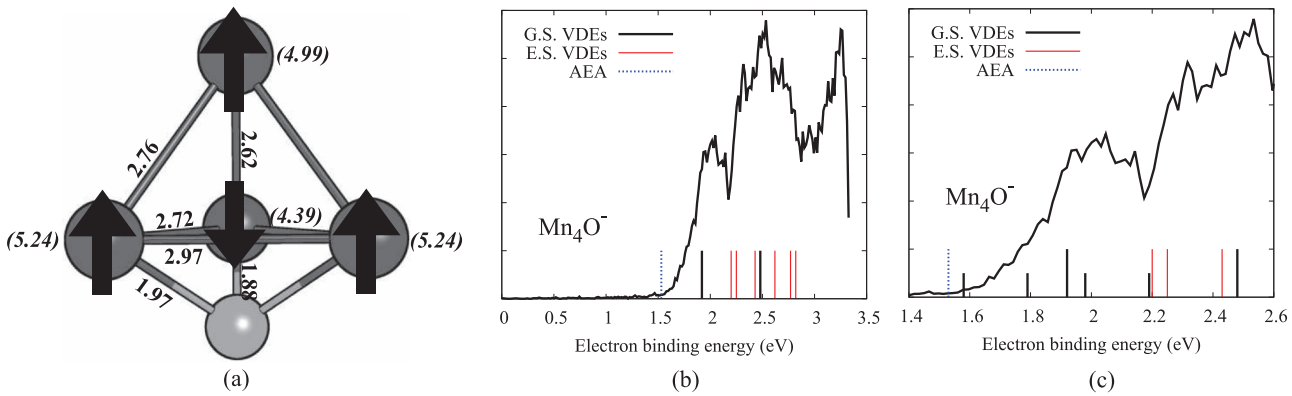

FIG. 3. (a) Ground-state structure and (b) photoelectron spectra of Mn_4O^-. Notation for the VDEs and the zoomed version (c) is identical to that in Fig. 1.

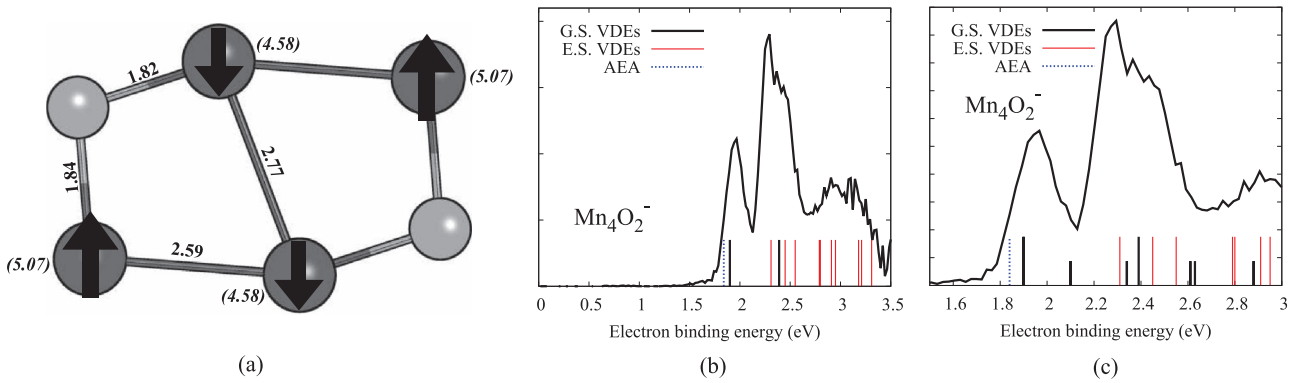

FIG. 4. (a) Ground-state structure and (b) photoelectron spectra of $Mn_4O_2^-$. Notation for the VDEs and the zoomed version (c) is identical to that in Fig. 1.

the in-plane isomag (12→11 and 12→13) are plotted in Fig. 3(b). The ground state VDEs and transitions to the first three excited states are shown along with the experimental PES in Fig. 3(b). The ground state VDEs show excellent agreement with the two primary spectral peaks, the adiabatic electron affinity lies directly at the start of the spectra, and the excited state values fall in the energy-window of the secondary features. Numerical values of these transitions are listed in Table I.

$Mn_4O_2^-$

The final cluster in our study is $Mn_4O_2^-$. With increasing cluster size comes the potential for many more low-lying structures. Optimization yields a global minimum with $M = 2$. Unlike Mn_4O^-, the lowest energy magnetic configuration is AFM, while the fM ($M = 12$) and FM ($M = 20$) arrangements are higher in energy by 0.63 and 1.20 eV, respectively. The ground state structure of $Mn_4O_2^-$ (Fig. 4(a)) is planar and resembles a Mn_2O^- dimer. The Mn-O bond distances, 1.82 Å and 1.84 Å, are close to that in Mn_2O^- (1.80 Å), and the cluster symmetry is C_{2h}. The presence of an additional oxygen reduces the overall cluster moment relative to Mn_4O^-. Nevertheless, the average Mn moment/atom is 4.83 μ_B, which is still close 5 μ_B. The anion with $M = 2$ has two anti-aligned moments and, hence, six possible spin configurations. Only three of these are non-degenerate, and the lowest energy isomag is shown in Fig. 4(a).

In calculating the VDEs, we consider the $M \pm 1$ transitions 2→1 and 2→3. Theoretical VDEs are again plotted with experimental PES in Fig. 4(b) and are listed in Table I. The first two sharp peaks are in very good agreement with the ground state VDEs. Additional features in the second peak correspond to transitions from the ground state of the anion to the excited states of the neutral, though there are likely other contributions to the spectra at high electron binding energies.

Neutral clusters and adiabatic electron affinities

We have also optimized the geometries of the neutral clusters, again stepping through all possible multiplicities. The ground state magnetic ordering of both Mn_3O and Mn_3O_2 are fM with $M = 6$. Mn_4O is also fM with $M = 11$, while Mn_4O_2 is AFM with $M = 1$. Just as with the anionic clusters, the neutral clusters have additional local minima corresponding to higher energy isomers. The global minimum for each is of greatest interest, as it allows calculation of the adiabatic electron affinity (AEA). This value can be estimated as the energy difference between the ground state of the anion and the ground state of the optimized neutral cluster. The AEAs for each cluster are shown in Table II. The calculated AEAs correlate well with the onset of spectral features in the PES data.

The explicit consideration of different isomags presented for the anions is repeated for the neutral clusters. During the time-scale of a vertical transition, we expect the electronic state to relax, enabling spins to reorient. Hence, the final spin configuration of the neutral cluster may be different from the anion, regardless of whether its geometry is held fixed or allowed to relax. Accurate VDEs and AEAs are achieved by applying our computational method to neutral clusters with fixed and relaxed geometries, respectively. The effect of spin relaxation on VDE energies is plotted in Figs. 1–4, where we include VDEs arising from transitions to higher energy isomags of the neutral (shown as shortened black lines in subfigure (c)). The structures, multiplicities, and relative energies of these isomags are provided in the supplementary material.[19]

Mn_3O has three higher energy isomags with unique energies. Transitions to these isomags from the ground state of the anionic cluster have VDEs of 1.56, 1.63, and 1.84 eV. These are plotted together with the lowest energy isomag VDEs in Fig. 1(c). The transition at 1.56 eV corresponds to a slight rise in intensity in the shoulder of the first peak, while the feature at 1.63 eV is very close to the ground state VDE given in Table I. The 1.84 eV correlates well with broadening to the right of the first peak.

TABLE II. Adiabatic electron affinity for the transition "relaxed anion→relaxed neutral."

Cluster	Transition	AEA (eV)	Expt. (eV)[a]
Mn_3O	7→6	1.50	1.56
Mn_3O_2	5→6	1.29	1.22
Mn_4O	12→11	1.53	1.42
Mn_4O_2	2→1	1.84	1.56

[a]Experimental values are estimated from the onset of EBE intensity and have an uncertainty of ±0.1 eV.

Similarly, Mn_3O_2 has three additional non-degenerate isomags, which are plotted in Fig. 2(c). Their VDEs are 1.40, 1.62, and 1.82 eV. All three VDEs are below the apex of the first peak, contributing to low-energy features in the experimental PES spectra. In the Mn_4O cluster, there are four additional isomags to consider (Fig. 3(c)). They correspond to VDEs of 1.58, 1.79, 1.98, and 2.19 eV. The effect of these transitions is a broadening of the low-energy shoulder and splitting of the first peak into three distinguishable sub-peaks. These effects are restricted to the low-energy regime; higher energy features are still described by transitions to the ground state or excited states only.

Finally, we find five higher energy, non-degenerate isomags for Mn_4O_2. The additional VDEs (plotted in Fig. 4(c)) are 2.10, 2.34, 2.61, 2.63, and 2.88 eV. This cluster is different from the other three in that none of the added VDEs lie below the ground-state values given in Table I. Instead, they intermingle with the energies of the excited state VDEs and cause broadening predominately in the second and third peaks. The first peak rises sharply and appears to be dominated by transitions to the neutral ground state only.

For all four clusters considered, additional transitions to higher energy neutral isomags correlate well with spectral broadening and with the presence of low-energy features at the onset of the spectra. Similar behavior is seen for Mn_2O, where the close energy of FM and AFM spin states causes vertical transitions from both isomers to coexist in the PES spectra.[10] As discussed by Khanna and co-workers, vertical transitions to higher energy isomers or isomags may occur in the course of the experiment without contributing significantly to the spectra because of lower transition probability. Therefore, the extent of peak broadening depends on transition probability (which is not considered in this work) and the energy difference between the isomags. Nearly degenerate isomags, as in the case of Mn_3O, produce sharp, narrow peaks, while systems with widely spaced isomags, such as Mn_4O, exhibit a gradual rise in PES intensity. Careful consideration of geometries and their different isomags is critical for accurate calculations of magnetic clusters.

CONCLUSION

In summary, we have calculated the optimized geometry and spin configuration of several manganese oxide (Mn_xO_y: $x = 2, 3, 4$, $y = 1, 2$) clusters using spin-unrestricted DFT. We have fully optimized the anionic species and used the lowest energy isomags to calculate the VDEs. Our theoretical ground-state VDEs match the experimental PES peaks reasonably well, and excited state calculations using TD-DFT show a general agreement with high-energy features of the spectra. Furthermore, we find that transitions from only one spin multiplicity contribute to each spectra, but that vertical transitions to multiple, non-degenerate isomags can explain low-energy features, such as peak broadening at the low-energy onset of the spectra. This supports the conclusion of Khanna *et al.*[10] and Jones *et al.*[11] that multiple isomags of Mn_xO_y clusters contribute to the PES spectra and that PES is a reliable technique for identifying spin isomers that may be undetected in conventional magnetic experiments. The presence of oxygen influences the overall cluster moment and spin configuration; ferrimagnetic and antiferromagnetic isomers are stabilized relative to the preferred ferromagnetic ordering of bare Mn_3 and Mn_4. This leads to ground state clusters with reduced net magnetic moments and, with the exception of Mn_3O^-, smaller Mn atomic moments as well.

ACKNOWLEDGMENTS

This work was supported by the Defense Threat Reduction Agency through the Advanced Energetics Initiative. K.W. acknowledges the support provided by the Office of Naval Research through its Naval Research Enterprise Intern Program.

[1] J. Mejía-López, A. H. Romero, M. E. Garcia, and J. L. Morán-López, Phys. Rev. B **78**, 134405 (2008).
[2] S. K. Nayak and P. Jena, Chem. Phys. Lett. **289**, 473 (1998).
[3] S. Paul and A. Misra, J. Mol. Structure: THEOCHEM **907**, 35 (2009).
[4] S. K. Nayak, B. K. Rao, and P. Jena, J. Phys.: Condens. Matter **10**, 10863 (1998).
[5] P. Bobadova-Parvanova, K. A. Jackson, S. Srinivas, and M. Horoi, J. Chem. Phys. **122**, 014310 (2005).
[6] M. Pederson, F. Reuse, and S. N. Khanna, Phys. Rev. B **58**, 5632 (1998).
[7] J. Jellinek, P. H. Acioli, J. Garcia-Rodeja, W. Zheng, O. C. Thomas, and J. Kit H. Bowen, Phys. Rev. B **74**, 153401 (2006).
[8] M. Qing-Min, X. Zun, L. Ying, and L. You-Cheng, Chin. Phys. Lett. **24**, 1908 (2007).
[9] S. N. Khanna, B. K. Rao, P. Jena, and M. Knickelbein, Chem. Phys. Lett. **378**, 374 (2003).
[10] S. N. Khanna, P. Jena, W.-J. Zheng, J. M. Nilles, and K. H. Bowen, Phys. Rev. B **69**, 144418 (2004).
[11] N. O. Jones, S. N. Khanna, T. Baruah, M. R. Pederson, W.-J. Zheng, J. M. Nilles, and K. H. Bowen, Phys. Rev. B **70**, 134422 (2004).
[12] S. K. N. P. Jena, J. Am. Chem. Soc. **121**, 644 (1999).
[13] M. J. Han, T. Ozaki, and J. Yu, J. Chem. Phys. **23**, 034306 (2005).
[14] B. K. Rao and P. Jena, Phys. Rev. Lett. **89**, 185504 (2002).
[15] G. L. Gutsev, S. N. Khanna, and P. Jena, Phys. Rev. B **62**, 1604 (2000).
[16] M. J. Frisch, G. W. Trucks, H. B. Schlegel *et al.*, GAUSSIAN 09, Revision A.1, Gaussian, Inc., Wallingford, CT, 2009.
[17] M. Gerhards, O. C. Thomas, J. M. Nilles, W.-J. Zheng, and J. K. H. Bowen, J. Chem. Phys. **116**, 10247 (2002).
[18] O. C. Thomas, W. Zheng, and K. H. Bowen, J. Chem. Phys. **114**, 5514 (2001).
[19] See supplementary material at http://dx.doi.org/10.1063/1.3698279 for additional information on magnetic and structural isomers.